Proceedings World Geothermal Congress 2020+1
Reykjavik, Iceland, April - October 2021

Systematic and Multidisciplinary Exploration in the Lithotopos - Iraklia Low Enthalpy Geothermal Field (Macedonia, Northern Greece)

Apostolos Arvanitis, Konstantina Kavouri, Georgios Vougioukalakis, Petros Karmis, Markos Xenakis, Ilias Koufogiannis, Vassiliki Somataridou, Panagiotis Vakalopoulos and Dimitrios Exioglou

Hellenic Survey of Geology and Mineral Exploration (H.S.G.M.E.), 1 Sp. Louis St., 13677 Acharnae, Greece

arvanitis@igme.gr, kkavouri@igme.gr, gvoug@igme.gr, karmis@igme.gr, markxen@igme.gr, ikoufogiannis@igme.gr, vsomataridou@igme.gr, vakalo@igme.gr, dimitrisexioglou@igme.gr

Keywords: geothermal exploration, multidisciplinary surveys, low enthalpy field, production wells, Strymon basin, Greece

ABSTRACT

The Lithotopos-Iraklia low enthalpy geothermal field is located in the NW part of the Strymon basin (Macedonia, Northern Greece) between Lake Kerkini and the small city of Iraklia. Ten exploration boreholes (Li-1 to Li-10) and one large-diameter exploration well (Li-1P) were drilled by I.G.M.E. in the period 1982-1983 and 2000 respectively, demarcating an area of about 45 km^2, which was officially characterized as 'probable low temperature geothermal field'. The temperatures of 40-62^{o}C were measured at depths of 200-433m. During 2013-2018, a systematic and multidisciplinary geothermal exploration was conducted by I.G.M.E. This geothermal project was divided into two main stages: (I) At first, a preliminary study was performed aiming at the definition of the locations of new production wells and included (i) collection and critical review of the existing geological, structural and drilling data, (ii) water temperature measurements, (iii) water sample collection and chemical analysis, (iv) soil gas (CO_2 and Rn) measurements and (v) geophysical surveys (TEM). (II) The appraisal study was the next development phase and included (i) drilling activities and construction of four production wells, (ii) borehole temperature measurements, (iii) assessment of thermal conditions, (iv) logging surveys, (v) pumping tests, (vi) determination of production capacity of wells, (vii) evaluation of hydraulic characteristics of the geothermal reservoir, (viii) distribution of productive aquifers, (ix) temperature and pressure distribution, (x) reservoir engineering and modeling approach, (xi) delineation of production and re-injection areas, (xii) water and gas sampling and analysis, (xiii) fluid geochemistry and geothermometry and (xiv) evaluation of scaling and corrosion potential of fluids. The obtained data is used to confirm the existence of geothermal resources suitable for future exploitation. Geothermal waters of up to 75^{o}C are hosted in sands, sandstones, conglomerates, breccias and fractured metamorphic basement. The new production wells, 352.5-519.5m deep, yield waters of 37.5-74.5^{o}C. The flow rates range between 5 and 80 m^3/h depending on lithology, aquifer properties and screen depths. The produced geothermal waters with TDS values of 0.55-1.32 g/l belong to the Na-HCO_3 type. The total installed thermal capacity from the existing production wells is estimated to be 4.47 MWt.

1. INTRODUCTION

The Lithotopos-Iraklia low enthalpy geothermal field is located in the NW part of the Strymon basin (Macedonia, Northern Greece) between Lake Kerkini and the small city of Iraklia. The Strymon basin is a typical post-orogenic graben of geothermal interest and important low temperature geothermal fields have been identified at the basin margins due to the favorable geothermal conditions: (i) intense and active extensional tectonics associated with large, deep and open normal faults through which hot fluids can circulate and rise to relatively shallow and exploitable depths or to the surface, (ii) crustal thinning, (iii) increased regional heat flow, (iv) Tertiary magmatism (granitoid intrusions), (v) existence of breccias and conglomerates on the top of the fractured basement and as interbedded strata and (vi) presence of an impermeable cap consisting of Neogene - Quaternary marly and clayey sediments (Arvanitis, 2003).

Based on the existence of an artesian well, 260m deep, which produced waters of 35-37.5^{o}C, ten (10) exploration boreholes (Li-1 to Li-10) were drilled by I.G.M.E. (Institute of Geology and Mineral Exploration) during 1982-1983 (Figure 1). Their depths range between 73 and 433m. The temperatures of 40-62^{o}C were measured at depths of 200-433m in sandstones and conglomerates close to the basement. The values of the average geothermal gradient for these exploration boreholes ranged from 2.3^{o}C/100m (Li-3) to 10.7^{o}C/100m (Li-4). Only three (3) exploration boreholes (Li-1, Li-3 and Li-7) reached and penetrated the metamorphic basement (Karydakis and Kavouridis, 1984; Karydakis et al., 2005). This drilling project has demarcated an area of about 45 km^2, which was officially characterized as 'probable low temperature geothermal field' (based on the new Geothermal Law, i.e. L. 4602/2019, this field is characterized as 'geothermal field of local interest'). In 2000, one large-diameter exploration well (Li-1P), 362m deep (Figure 1), was constructed by I.G.M.E., the bottom-hole temperature of 48^{o}C was measured but pumping tests were not carried out (Karydakis et al., 2001; Karydakis et al., 2005). The rights to explore the Lithotopos-Iraklia low temperature geothermal field have been leased to the Municipality of Iraklia since 2010.

In the period 2013-2018, a systematic geothermal investigation was carried out by I.G.M.E. under a contract made between I.G.M.E. and the Municipality of Iraklia. The geothermal project was divided into two main stages: (I) At first, a preliminary study was performed aiming to define the locations of new production wells and included (i) collection and critical review of the existing geological, structural and drilling data, (ii) water temperature measurements, (iii) water sample collection and chemical analysis, (iv) soil gas (CO_2 and Rn) measurements and (v) geophysical surveys (TEM). (II) The appraisal study was the next development phase and included (i) drilling activities and construction of four production wells, (ii) borehole temperature measurements, (iii) assessment of thermal conditions, (iv) logging surveys, (v) pumping tests, (vi) determination of production capacity of wells, (vii) evaluation of hydraulic characteristics of the geothermal reservoir, (viii) distribution of productive aquifers, (ix) temperature and pressure distribution, (x) reservoir engineering and modeling approach, (xi) delineation of production and reinjection areas, (xii)

water and gas sampling and analysis, (xiii) fluid geochemistry and geothermometry, (xiv) evaluation of scaling and corrosion potential of fluids and (xv) estimations of the thermal energy of the produced geothermal waters with the corresponding installed thermal capacity. This exploration project was entirely funded by the Municipality of Iraklia.

2. GEOLOGICAL, TECTONIC AND HYDROGEOLOGICAL SETTING

Geologically, the area belongs to the Vertiskos series of the Serbo-Macedonian Massif (SMM). The metamorphic basement (Figure 1) mainly consists of bi-mica and mica gneisses, leucocratic and augen gneisses, amphibolite gneisses, amphibolites, alternations of gneisses and amphibolites, schists, quartzites, pegmatite-aplite veins and migmatites (small outcrops of the meta-ultrabasic rocks). Ophiolitic bodies (peridotites, mostly serpentinized) are in a tectonic unconformity to the surrounding gneisses (Staikopoulos et al., under publication). The basement is intensively fractured. Sulphate-bearing coatings occur sporadically on weathered rock surfaces.

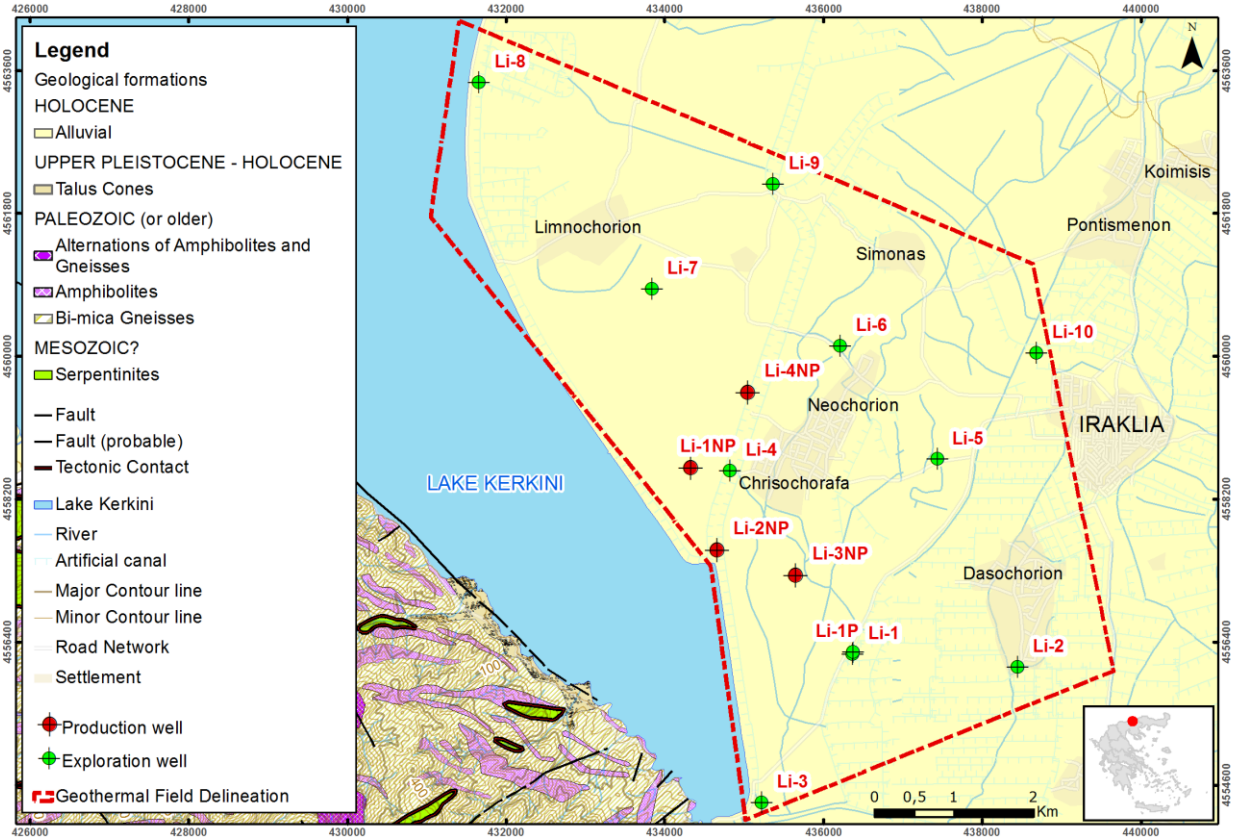

Figure 1: Geological map of the Lithotopos - Iraklia geothermal area.

Neogene (Pliocene) - Quaternary terrestrial, fluvio-terrestrial, fluvio-torrential and fluvial marsh sediments overlay the basement (Figure 1). The Plio-Pleistocene terrestrial and fluvio-torrential sediments consist of red beds with mainly rubbles of gneissic, quartzose, amphibolitic composition and less grits, sands and clays. Unconsolidated scree and talus cones composed of cobbles and rubbles of various sizes, gravels, sands, clayey sands and clays occur west and northwest of Lake Kerkini. The Holocene sediments consist of marsh deposits (clays, clayey sands, loams and loamy sands of dark grey to black color due to organic material), alluvial sediments (silts, clays, sandy clays, terra rossa, clayey sands, sands with dispersed gravels) and fluvial - torrential deposits (sands, sandy clays, loamy sands, loams, grits, pebbles) (Staikopoulos et al., under publication). The sedimentary sequence of the area can be divided into two main Units: (a) a Lower Unit of Plio-Pleistocene age (terrestrial and fluvial deposits), with an average thickness of about 200m (maximum thickness: 252m), composed of brownish-yellowish sediments (fine to medium-grained sandstones with interbedded gravels and clays) and red beds and (b) an Upper Unit (fluvial and marsh deposits), with an average thickness of about 200m (thickness range: 150-300m), consisting of coarse to fine-grained sands, intercalated dark grey-green clays and rounded gravels.

The main fault systems are generally oriented NW-SE and NE-SW (Figure 1). During the Quaternary, the new active extensional regime with N-S tensional direction formed a new group of normal E-W faults and reactivated pre-existing faults. The large high-angle NW-SE normal fault located along the longitudinal axis of Lake Kerkini is an important tectonic structure between basement and basin sediments which delineates the western margin of the Strymon basin and affects the geothermal conditions of the area (Arvanitis, 2019). Other smaller scale normal faults parallel to this major tectonic structure cut the metamorphic basement and cataclastite zones occur along some of them. Small antithetic NW-SE trending and SW-dipping faults have been observed at some locations. East of Lake Kerkini, the basement gradually subsides eastwards due to NW-SE trending and NE-dipping syn-sedimentary normal faults. Some NE-SW normal faults cut across the NW-SE striking faults. East of Lake Kerkini, NW-SE, NE-SW and E-W normal faults are covered by the Pliocene-Quaternary sediments and their probable presence and location are detected by geophysical methods. During the Quaternary, a new and active extensional regime with N-S tensional direction formed a new group of roughly E-W trending normal faults and reactivated pre-existing faults.

The hydrogeological behavior of the geological formations depends on their lithology and tectonic features. The basement is composed of impermeable metamorphic rocks but the intense fracturing and faulting create a secondary permeability and favor water circulation. The Pliocene-Quaternary sediments are characterized as permeable/semi-permeable formations. Sandstones, sands, gravels, pebbles and rubbles form the water-bearing strata. The Quaternary deposits (sands, gravels) of the Upper Unit of the sedimentary sequence are characterized by moderate to high permeability, while the sandstones, sands, gravels, pebbles and rubbles of the Lower Unit have low to moderate permeability. Scree and talus cones have high permeability and host good water-yielding aquifers due to their coarser grained character. Almost all groundwater wells are artesian.

3. SOIL GAS MEASUREMENTS

In order to draw some better conclusions about the best locations for new production wells in the Lithotopos-Iraklia geothermal field, soil gas sampling and measurements were performed in situ. The soil gas measurements were carried out using appropriate portable equipment and included the determinations of CO_2 flux, CO_2 concentrations and radon concentrations at specific sites. Carbon dioxide and radon constitute inert gases suitable for detection of active tectonic lines. The results of these measurements are illustrated in Figure 2 and showed that the area having higher values and being of primary interest is located around exploration borehole Li-4 and northeastwards.

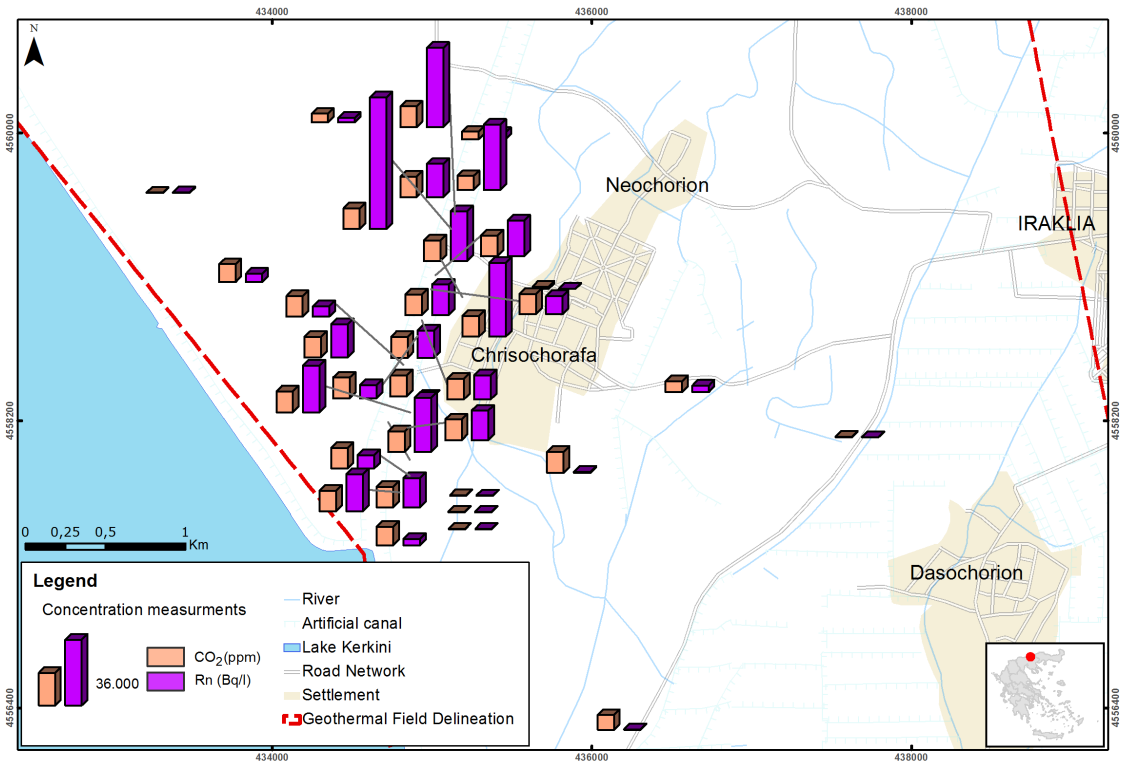

Figure 2: CO_2 and radon concentration measurements during the soil gas survey in the Lithotopos-Iraklia geothermal field.

4. GEOPHYSICAL SURVEYS

Geothermal exploration is a multidisciplinary task which entails various activities, among which geophysical surveys can play an important role to determining the existence of a geothermal resource and subsequently identifying suitable drilling sites. Electrical methods are the most widely used geophysical methods in the surface exploration of geothermal areas, since the parameter of interest is the electrical resistivity of the rocks which correlates both with the temperature and alteration of the rocks which are key parameters of the geothermal systems. Geothermal systems commonly contain saline fluids while hydrothermal alteration processes cause pervasive changes to the resistivity of the rocks in which the systems develop. In general, this salinity and clay alteration together with the high temperatures associated with geothermal activity tend to result in lower overall resistivity in geothermal systems. The resultant low resistivity anomalies have generally been the main target for geophysical exploration of geothermal resources. From the various types of electrical methods we used the Transient Electromagnetic method (TEM), where current is induced by a time varying magnetic field from a controlled source. The monitored signal is the decaying magnetic field at surface from the secondary magnetic field.

The objectives of the geophysical survey were: (i) to map the subsurface of investigation area in terms of the geoelectrical stratigraphy, (ii) to map the depth to the top of the metamorphic basement (gneiss) and to determine the structural discontinuities, (iii) to detect low resistivity anomalies attributed to the alteration clay zones capping the possible reservoir. The in-loop and coincident loop configurations were used with size of 200x200m.

A total of 74 TEM soundings were measured and the data were inverted with a 1D scheme assuming models of 4 to 5 layers, with the Terra software by Karmis (2003). The results of the inversions are presented in terms of geoelectrical layered models of resistivity and thickness.

Typical examples of the TEM soundings and interpretation models are shown in Figure 3. The geoelectric stratigraphy of all soundings indicate the presence of sediments with resistivity values between 6.5 and 33 Ohm*m to the depth of about 120 m. Below this depth, a conductive layer with resistivity values below 4 Ohm*m is present, overlying the resistive metamorphic basement. The resistivity values of the highly conductive layer are found in accordance with the results of electrical logging performed in production wells Li-1NP and Li-2NP. The high conductivity of this layer is attributed to clay alteration and geothermal fluids. Extremely high conductivity values were recorded at sounding 6, which was measured in the vicinity of well Li-2NP, where the maximum temperature was recorded.

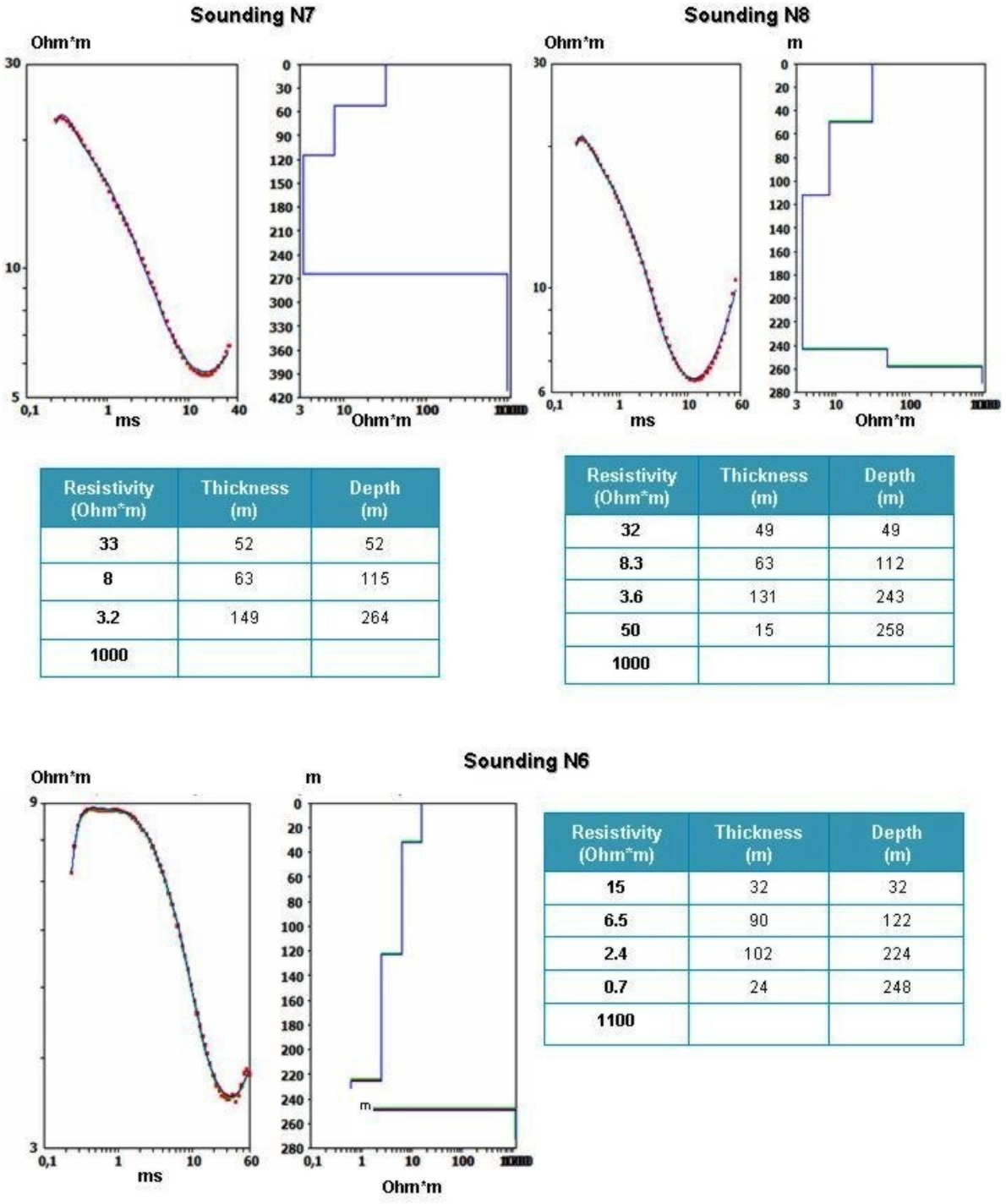

Resistivity (Ohm*m)	Thickness (m)	Depth (m)
33	52	52
8	63	115
3.2	149	264
1000		

Resistivity (Ohm*m)	Thickness (m)	Depth (m)
32	49	49
8.3	63	112
3.6	131	243
50	15	258
1000		

Resistivity (Ohm*m)	Thickness (m)	Depth (m)
15	32	32
6.5	90	122
2.4	102	224
0.7	24	248
1100		

Figure 3: Inversion results and interpretation models of soundings N7, N8 and 6. The location of soundings is shown in Figure 4.

The validity of interpretation of the TEM soundings was verified by the drilling results of wells Li-1NP, Li-2NP, Li-3NP and Li-4NP. The isodepth map (Figure 4) of the depth to the top of the metamorphic basement was compiled by the results of the TEM survey along with the drilling results. From geological observations and the geophysical evidence deduced by the TEM survey the position of two main structural discontinuities oriented NW-SE and NE-SW can be deduced. East of Lake Kerkini the depth to the basement increases by 300-400m due to the NW-SE faults. Local depressions and uplifts of the basement are detected due to the presence of small NE-SW faults.

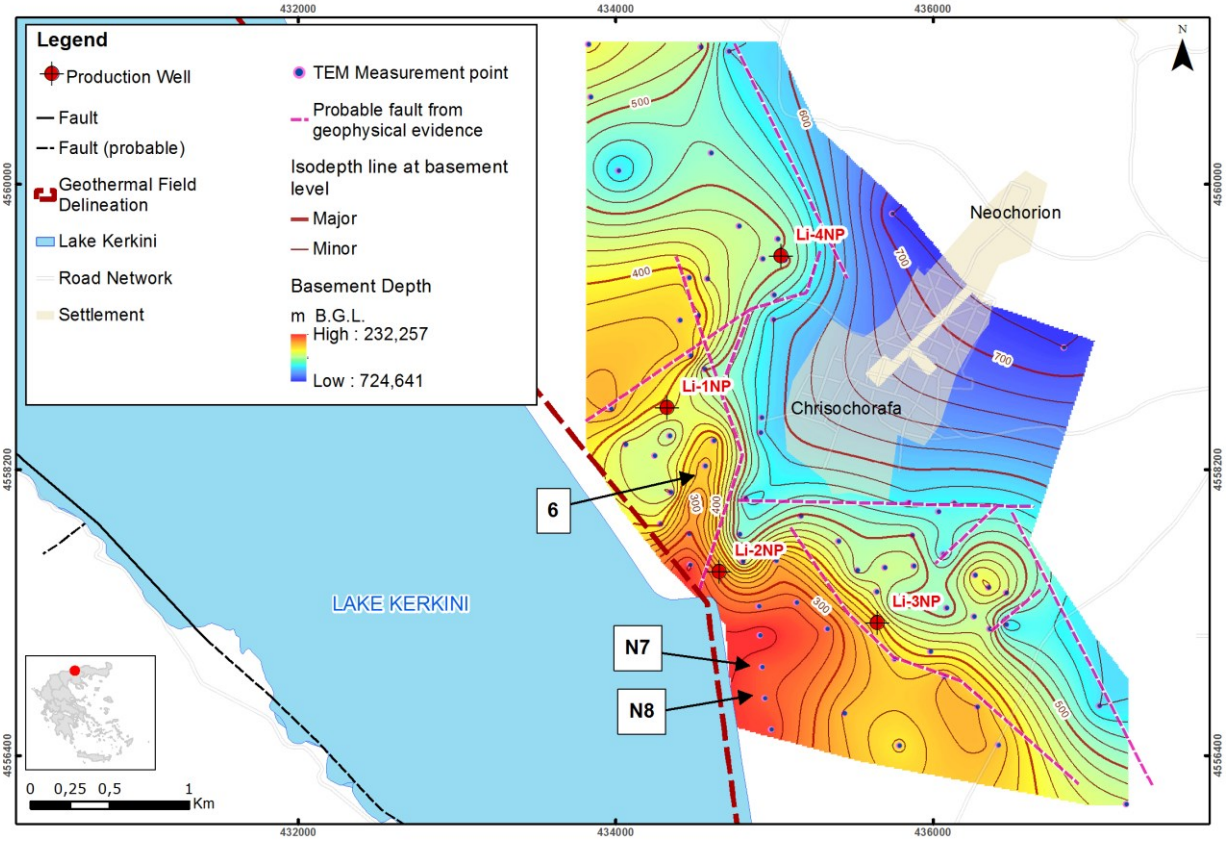

Figure 4: Isodepth map of the top of the metamorphic basement based on the results of geophysical surveys (TEM) and drilling activities. Probable normal faults detected by geophysical surveys are drawn as dashed lines. TEM measurement sites are illustrated as dots.

5. PRODUCTION WELLS

Drilling works were carried out during the period 2016-2018, resulting to four (4) production wells: Li-1NP, Li-2NP, Li-3NP and Li-4NP (Figures 1, 4 and 5). The encountered geological formations consist of recent and Quaternary deposits of small thickness followed by sand and clay intercalations of the Upper sedimentary unit, then sandstone of the Lower sedimentary unit and finally the metamorphic rocks of the basement. All four geothermal wells present artesian flow and strongly positive geothermal gradient. Casing and screen were placed at the appropriate depths inside boreholes according to borehole logging suggestions, while upper aquifers were isolated with cement seal from the surface to approximately 250 m depths. During the construction of production wells, cold aquifers were completely isolated in geothermal wells Li-1NP, Li-2NP and Li-3NP and partly isolated in geothermal well Li-4NP. Fluid temperature was measured at intervals of 10 m from surface to the bottom of each well. Bottom hole temperatures range from 59 to 75°C. The temperature profiles of the production wells are presented in Figure 6.

In order to determine the potential of the constructed geothermal wells and the hydraulic characteristics of the geothermal reservoir, step-drawdown and 24h constant yield pumping tests were conducted successively at each well. A submersible pump, suitable for temperatures up to 90°C, was placed inside the well at 152.5 m depth. Flow rates and exit temperatures were measured with digital flow meter and digital thermometer respectively. Water level inside the pumped well was gauged systematically, while one data logger for both temperature and pressure was placed inside the piezometric tube at 80 m depth. At least one nearby well was monitored during the pumping tests.

During the course of pumping, the exit temperature of geothermal fluids raised by 2°C at Li-1NP, by 3°C at Li-2NP and by 15°C at Li-3NP, while at Li-4NP no change was marked. Data was processed in the AquiferWin32 software, in respect to the Theis method (Theis, 1946) and Cooper-Jacob solution (Cooper and Jacob, 1946) for constant yield pumping and Eden-Hazel solution for step-drawdown tests (Eden and Hazel, 1973). The hydraulic and thermal characteristics of the newly constructed geothermal wells are resumed in Table 1.

The geothermal fluids identified by the present drilling operations present temperatures from 59.3 to 75°C in economically exploitable depths. The temperature of 75°C measured at geothermal well Li-2NP, is so far the maximum temperature identified in the Strymon basin. Production rates vary from 5 to 80 m³/h depending on the hydraulic characteristics of the pumped aquifer and the construction specifications of each well. High production rates of well Li-4NP are attributed to the partial isolation of overlying cold aquifers and are related to lower exit temperatures. In general, the conducted pumping tests indicate very low values of hydraulic conductivity, at the order of 10^{-7} to 10^{-8} m/s.

Table 1: Hydraulic and thermal characteristics of new geothermal production wells

Geothermal well	Li-1NP	Li-2NP	Li-3NP	Li-4NP
Depth	417.3 m	352.5 m	383 m	519.5 m
Exit Temperature	52.5°C	73.5°C	59°C	37.5°C
Reservoir Temperature	62°C	75.0°C	66.5°C	59.3°C
Wellhead pressure	0.6 bar	0.8 bar	0.2 bar	0.4 bar
Artesian discharge Q_a	4 m³/h	15.5 m³/h	1.5 m³/h	25 m³/h
Production rate Q_p	15 m³/h	45 m³/h	5 m³/h	80 m³/h
Drawdown s	78 m	115 m	98 m	7.5 m
Hydraulic conductivity K	$5\ 10^{-7}$ m/s	$7.5\ 10^{-7}$ m/s	$6.9\ 10^{-8}$ m/s	$1.4\ 10^{-7}$ m/s
Transmissivity T	$3.04\ 10^{-5}$ m²/s	$6.77\ 10^{-5}$ m²/s	$6.67\ 10^{-6}$ m²/s	$2.7\ 10^{-5}$ m²/s
Radius of influence	<498 m	<1,015 m	<1,044 m	<1,014 m

6. GEOTHERMAL RESOURCE CHARACTERISTICS AND MODELING

The results of the present exploration campaign, as well as previous investigation in the Lithotopos-Iraklia geothermal field (Karydakis and Kavouridis, 1984), are combined to a three dimensional model, using the FEFLOW code for flow and heat transport in porous and fractured media (Diersch, 2014).

The hydrogeological model is characterized by a quasi-permeable sedimentary sequence of a minimum 230 m to a maximum 720 m of thickness, which overlies the impermeable metamorphic rocks of the basement. The upper sedimentary unit has good permeability and contains cold aquifers that become slightly warmer in depth. The lower sedimentary unit consists of sandstone with variable mineralogical composition, grain size distribution and thickness. The values of hydraulic conductivity calculated for this unit with both analytical and numerical methods, reveal a low permeability formation. This unit constitutes the main geothermal resource of the Lithotopos-Iraklia geothermal field. The impermeable basement of the hot aquifer consists of metamorphic rocks, mainly gneiss and amphibolite. Locally, it is intensively fractured and presents hydrothermal alterations. The geometry of the metamorphic basement is affected by NW-SE trending normal faults, resulting to a steep dipping towards NE.

Following the variable sediment deposition at the different parts of the basin, the spatial distribution of hydraulic conductivity is non-uniform. Fluid flow is mainly controlled by faults of NNE-SSW direction that transect the sedimentary basin. Hydraulic head measurements both at deep and shallow wells, indicate that the reservoir is not completely capped at the top, which is also supported by the lack of a distinct impermeable layer between the upper and lower sedimentary units. Consequently, geothermal fluid leaks towards upper aquifers, causing different waters to mix and heat to transfer via convection. At the west part of the geothermal field, hydraulic pressures of all aquifers balance at the mean water level of Lake Kerkini which constitutes a very important water boundary in the area. In regional scale, hydraulic heads decrease smoothly as we move away from the lake following a general flow direction from SW to NE.

Water temperature measurements at different depths were analyzed in order to determine abnormal temperature patterns and locate probable heat sources. Shallow aquifers (up to 200 m depth) present a positive heat anomaly in the SSW part of the geothermal field. The higher temperature encountered at this depth is 42°C. At depths greater than 300 m, the maximum temperature of 75°C has been recorded in geothermal well Li-2NP, near the east bank of Lake Kerkini. Isothermal contours at the depth of 300 m are presented in Figure 5.

The area around geothermal well Li-2NP is characterized by the highest temperatures and hydraulic heads of the geothermal field and is considered to be the close to the upflow zone of the geothermal system. Geothermal fluid, which originates from greater depths, rises following the conductive paths of major faults of the basement. Then, it diffuses in the sediments of the basin and forms the geothermal resource of the Lithotopos - Iraklia geothermal field. Based on the shape of the isothermal contours and taking into account (a) the basement faults detected by geophysical surveys and (b) the geothermal conditions in other parts of the western margin of the Strymon basin, it is assumed probable that the geothermal fluids rise mostly through the large NW-SE normal fault located along the longitudinal axis of Lake Kerkini while the NE-SW and E-W faults favor the fluid flow and the extension of the geothermal anomaly eastwards (Figure 5). The geothermal anomaly decreases gradually from west (east bank of Lake Kerkini) to the east. Additionally, local anomalies at the piezometric and temperature fields are related to the geometry of the basement and the local development of clay lenses. A three dimensional aspect of the geometry and temperature distribution of the Lithotopos geothermal field is presented in Figure 6.

Thermal conductivity and specific heat capacity of the geothermal fluid are the same as for water, i.e. 0.65 W/mK and 4.2 MJ/kgK respectively. For each hydrolithological unit the thermal properties of solids are calculated in respect to principal mineralogical composition, porosity and water saturation for temperatures up to 80°C. The upper sedimentary unit is divided in two layers, a shallow (L1) and a deeper (L2), according to whether temperatures higher than 30°C are observed (30ºC is the limit for geothermal potential characterization based on the new Greek Geothermal Law). The calculated values for all hydrolithological units are presented in Table 2.

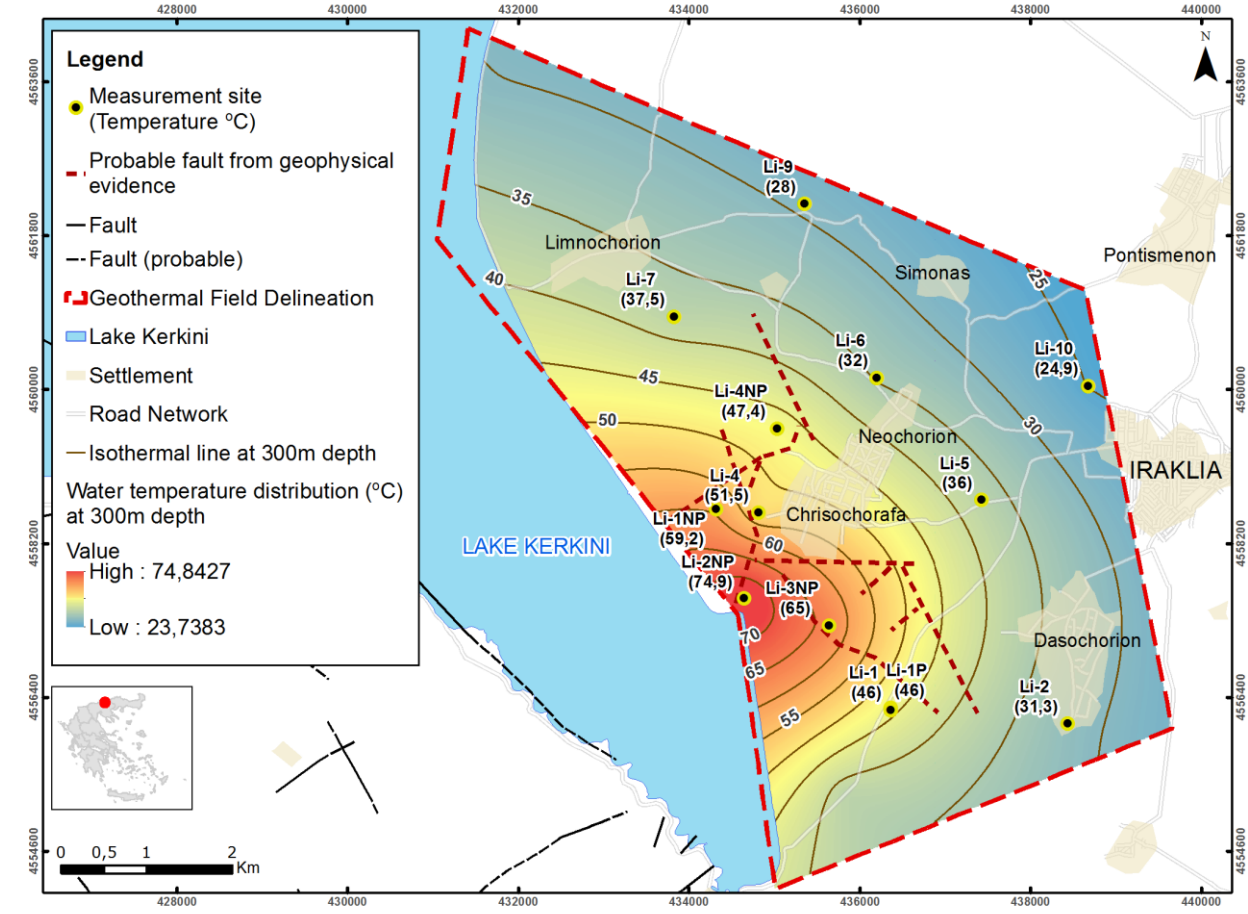

Figure 5: Water temperature distribution at the depth of 300 m.

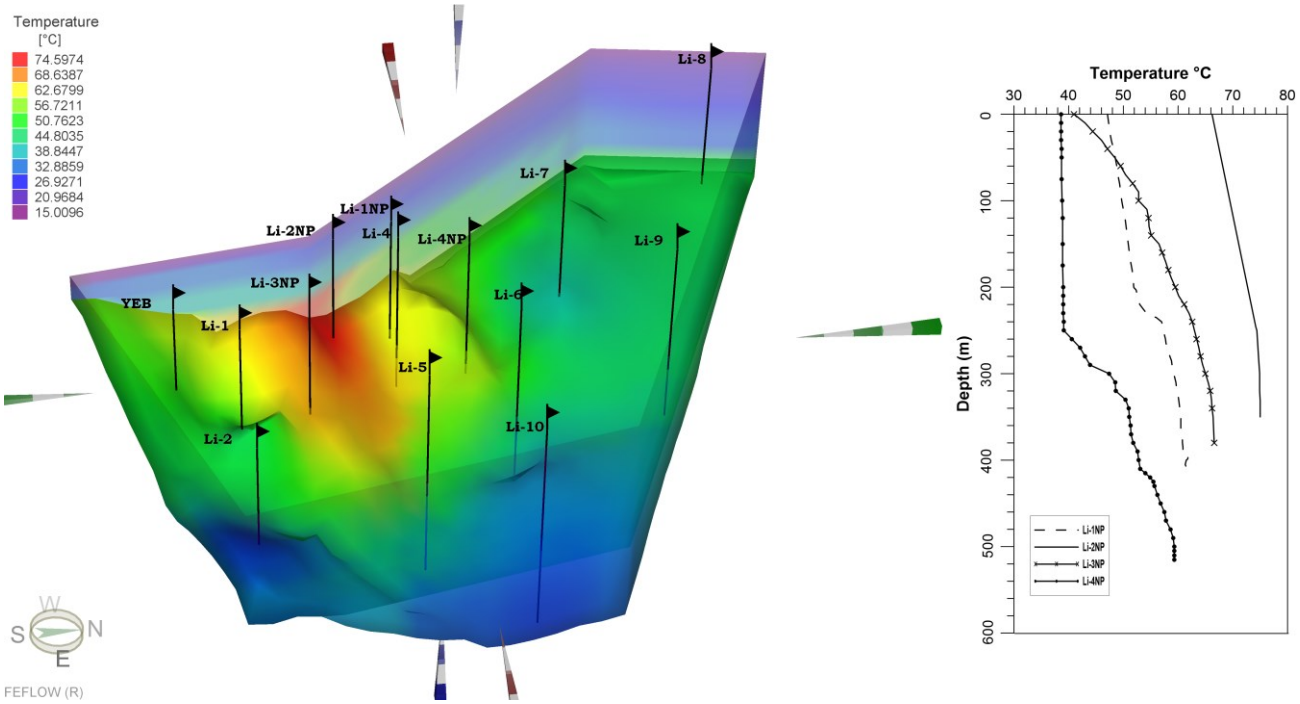

Figure 6: (Left) Three dimensional aspect of the geometry and temperature distribution of the Lithotopos-Iraklia geothermal field. (Right) Temperature profiles of production wells Li-1NP, Li-2NP, Li-3NP and Li-4NP.

Table 2: Thermal properties of solids

Hydrolithological Unit	Thermal conductivity (W/mK)	Specific heat capacity (MJ/kgK)
Upper sedimentary unit shallow (L1)	2.44	1.9
Upper sedimentary unit deep (L2)	3.7	2
Lower sedimentary unit	2.9	2.64
Metamorphic basement	3.4	1.6

7. FLUID GEOCHEMISTRY

Water sampling was carried out in the area, with emphasis given on systematic sampling during the pumping and recovery tests of the four production wells. A number of representative samples of thermal and cold waters coming from older exploration wells (Karydakis et al., 2005) were taken into account for comparison. Temperature, pH, Eh, conductivity, dissolved ^{222}Rn and dissolved CO_2 were measured in situ, as appropriate. Eh measurements are used to show qualitative trends but cannot be interpreted as equilibrium values. Filtered (0.45 μm), acidified (with HNO_3 Suprapur) water samples were collected for determination of cations and SiO_2. Untreated samples were collected for analyses of anions. Chemical analyses were conducted at the Analytical Laboratories of H.S.G.M.E., using mainly ICP and spectrophotometry. Dissolved ^{222}Rn was determined with SARAD device. ^{226}Ra was measured via radon emanation technique. Dissolved CO_2 was estimated by titration with Na_2CO_3 N/22. Gas measurements were carried out in situ with CROWNCON T–4 and DRAGER X.am7000 devices. Gas sampling was carried out in well Li-2NP during artesian flow. Gas chromatography analysis was carried out at the Laboratory of the Chemical Engineering Department of the Aristotle University of Thessaloniki. Water analyses results are given in Table 3.

Table 3: Main physical and chemical parameters of the water samples studied.

No.	Well Name	Sampling Date	X GGRS '87)	Y GGRS '87)	Flow rate (m^3/h)	Eh (mV)	pH	T (°C)	TDS (mg/l)	Na^+ (mg/l)	K^+ (mg/l)	Mg^{2+} (mg/l)	Ca^{2+} (mg/l)
1	Li-1NP	18/10/18	434320.20	4558592.50	4	n/a	8.24	47	910	323	27.62	8.30	9.82
2	Li-1NP	16/10/18	434320.20	4558592.50	20	n/a	7.88	53.1	1310	400	42.53	8.99	12.07
3	Li-2NP	22/10/18	434651.50	4557556.80	45	-160	7.83	74	1301	421	49.92	4.66	12.61
4	Li-2NP	23/10/18	434651.50	4557556.80	15.5	n/a	7.85	70.1	1319	444	48.69	4.69	14.43
5	Li-3NP	18/10/18	435645.00	4557236.00	5	n/a	7.69	58.8	1161	393	37.23	3.09	15.53
6	Li-3NP	20/10/18	435645.00	4557236.00	1.5	-210	7.76	44.3	1205	417	41.07	3.09	15.35
7	Li-4NP	25/10/18	435040.00	4559548.00	80	n/a	8.12	37.4	549	178	11.99	10.76	10.95
8	LIM-1	21/04/83	433083.73	4561637.20	n/a	n/a	7.3	27.5	345.2	68	2.00	3.89	16.04
9	Lith-3	24/06/14	437241.00	4552108.00	n/a	n/a	7.46	15.4	276	12	4.02	26.90	42.10

No.	HCO_3^- (mg/l)	SO_4^{2-} (mg/l)	Cl^- (mg/l)	SiO_2 (mg/l)	F^- (mg/l)	Fe (mg/l)	Li (mg/l)	As (mg/l)	B (mg/l)	CO_2 (mg/l)	U (mg/l)	^{226}Ra (bq/l)	^{222}Rn (bq/l)
1	688.31	115.02	60.33	26.60	2.17	0.15	0.17	0.14	1.65	n/a	<0.005	0.05	3.94
2	828.65	170.04	83.01	40.10	2.90	1.26	0.23	0.02	2	20	<0.005	n/a	n/a
3	823.77	240.05	101.91	65.93	4.18	0.15	0.43	0.04	1.90	130	<0.005	0.02	13.75
4	821.33	235.05	101.69	66.62	4.30	0.09	0.42	0.06	1.85	n/a	<0.005	n/a	n/a
5	796.92	185.04	75.41	59.30	2.66	0.65	0.27	0.04	1.50	n/a	<0.005	n/a	n/a
6	827.43	185.04	80.91	63.30	3.74	0.10	0.29	0.05	1.50	90	<0.005	0.03	8.45
7	427.14	74.02	26.34	49.40	1.22	0.33	0.06	0.01	1	n/a	<0.005	0.07	7
8	173.90	49.00	8.87	21.60	0.05	n/a	n/a	n/a	n/a	n/a	<0.005	n/a	n/a
9	213.00	55.30	8.51	17.40	0.30	<0.01	<0.005	<0.005	0.04	n/a	<0.005	n/a	n/a

In Figure 7, water analyses are plotted on a Piper diagram (Piper, 1944; Powell, 2000). Na-HCO_3 type represents the thermal waters of the area, including those from the four production wells. Temperatures of produced waters range from 37.4 to 74°C, pH is slightly alkaline (7.69-8.24) and total dissolved solids (TDS) range from 549 to 1,319 mg/l. Cold waters fall under the Ca, Mg-HCO_3 type, with a representative sample recording temperature as low as 15.4°C, slightly alkaline pH of 7.46, plus 276 mg/l of TDS. Mixed water type displays intermediate thermal and chemical characteristics. A representative sample records 27.5°C, 7.3 pH, plus TDS content of 345.2 mg/l. The above observations indicate that there are mixing processes taking place in the system.

In situ gas phase measurements showed a mean ^{222}Rn concentration of 231000 Bq/m^3, i.e. remarkably higher than those recorded as dissolved ^{222}Rn in the waters, as a result of its migration to the gaseous phase. They also recorded the absence of H_2S, 0.013% CO, 0.04% H_2, 0.8% v/v O_2, 1.25% CH_4 and CO_2>5% (concentrations in % v/v).

Gas sample collected from Li-2NP well was dominated by N_2, which constituted the 62% v/v of total gases. The remaining fraction was found to be CO_2 (27% v/v) and CH_4 (11% v/v). The main hypothesis here is that the gas phase is a mixture of trapped atmospheric air with a proportion of CO_2 coming from the dissolution of calcite and sedimentary derived CH_4 produced due to the thermal breakdown of organic matter and inorganic synthesis (Etiope et al., 2007).

Various silica and alkali geothermometers were used in an attempt to estimate deep subsurface temperatures (Table 4). Applying geothermometry to a low-enthalpy geothermal system can raise controversies. Geothermal waters of the area are non-equilibrated (Figure 8), which means that the use of Na/K geothermometers would give misleading results (D'Amore, 1992; Giggenbach, 1988).

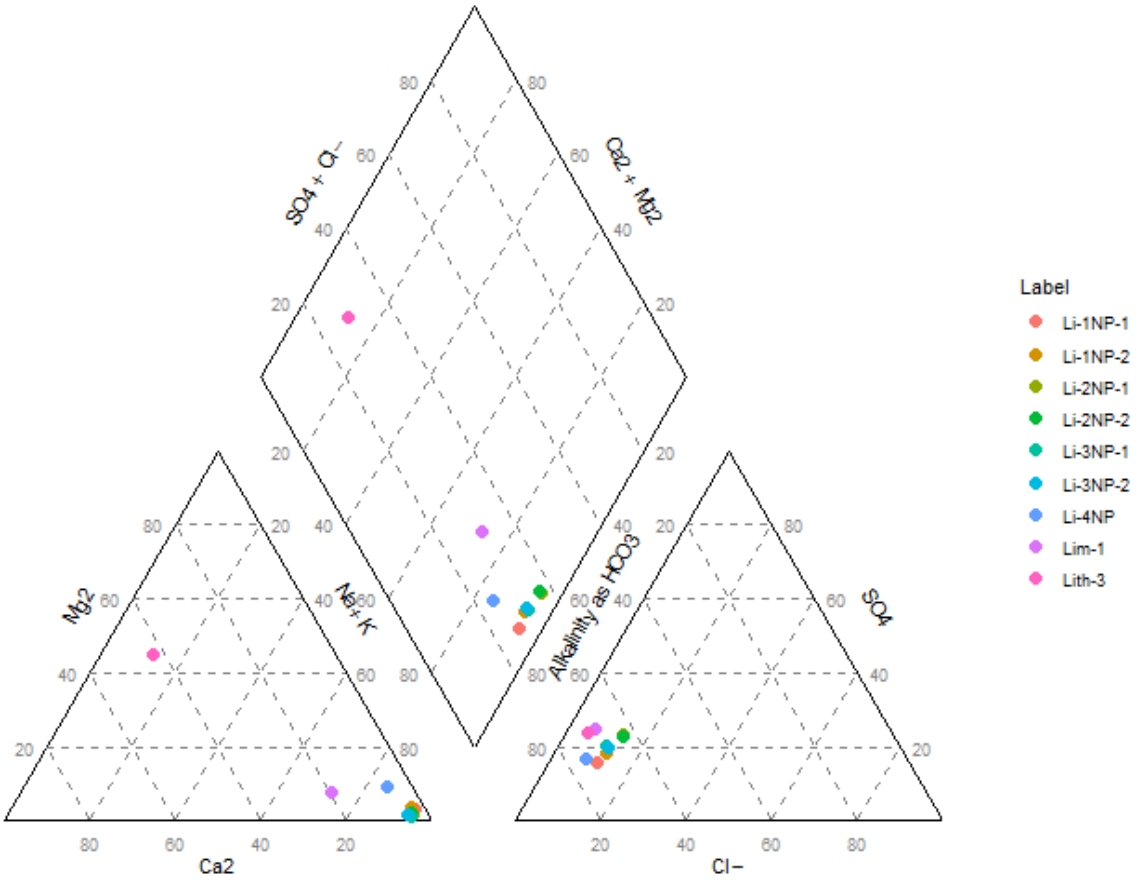

Figure 7: Chemical analyses of water samples studied are plotted on a Piper diagram.

Considering the field's structure, the characteristics of the waters, as well as the limitations in the use of each geothermometer, it is concluded that the chalcedony geothermometer (Arnórsson et al., 1983) gives the most reliable reservoir temperatures, which reach up to maximum value of 87°C for well Li-2NP. It is also notable that the Na/Li geothermometer gives temperatures close to the recorded ones, with the exception of the unreal negative value of Li-4NP well's sample. The thermometer is sensitive to mixing with cold water processes (Fouillac and Michard, 1981).

Table 4: Deep reservoir temperatures computed by some chemical geothermometers.

No.	Well Name	SiO_2 (Arnorsson et al. 1983)	Na-K-Ca Mg corr (Fournier and Pot er, 1979)	K/Mg (Giggenbach 1986)	Na/Li, Cl<0.3M (Fouillac and Michard 1981)
1	Li-1NP	43	40	95	44
2	Li-1NP	61	57	106	48
3	Li-2NP	86	112	120	74
4	Li-2NP	87	112	119	75
5	Li-3NP	81	124	117	57
6	Li-3NP	84	129	120	57
7	Li-4NP	71	19	71	-116

A qualitative scaling and corrosion potential estimation has been made. Langelier Saturation Index (LSI) and Ryznar Stability Index (RSI) served as predictive tools for $CaCO_3$ scale. Saturation Indexes (SI) of critical phases were calculated with PHREEQC (Parkhurst and Appelo, 2013). The corrosivity of the waters has been evaluated with the empirical Classification System suggested by Ellis (1981). This system is valid for waters with temperatures >49°C, thus water from Li-4NP is excluded. The parameters of TKS (Total Key Species), i.e. the sum of Cl^-, SO_4^{2-}, HCO_3^-, CO_3^{2-}, sulfide species and ammonia species in ppm, Cl^- fraction in TKS, pH and temperature are taken into account. Results are presented in Table 5.

LSI, RSI, and SI (calcite and aragonite) values demonstrate that the waters are close to equilibrium with respect to $CaCO_3$, implying a negligible concern about $CaCO_3$ scaling. The only case which showed some non-negligible scaling was Li-2NP, with heavy reddish – brown colored iron oxides also observed. Precipitation of iron compounds are predicted by PHREEQ calculations (Table 5). This, combined with the negative Eh measurements, indicate anaerobic well water, i.e. reducing environment, capable of either dissolving iron from the aquifer rock and the steel parts, or enabling iron compounds to be deposited in parts of the system that are exposed to aeration or mixed with waters that contain significant amounts of oxygen (Papic, 1991). Moreover, close to equilibrium SI values of chalcedony favor the use of chalcedony geothermometer.

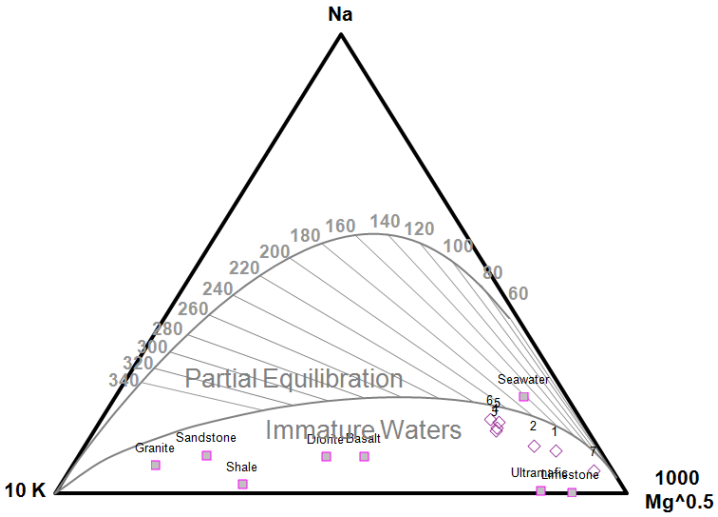

Figure 8: Chemical analyses of water samples studied are plotted on a Giggenbach diagram.

Corrosivity assessment showed that Lithotopos-Iraklia geothermal waters fall under Classes V_a and V_b, i.e. they can cause uniform corrosion plus some pitting corrosion. Under conditions like these, stainless steel (T316) is a suitable selection as construction material for the geothermal wells and installations.

Table 5: Factors calculated for scaling and corrosion prediction on the four productive wells.

No.	Well Name	LSI	RSI	SI calcite	SI aragonite	SI chalcedony	SI hematite	SI goethite	TKS (ppm)	Cl in TKS (%)
1	Li-1NP	0.46	6.97	0.39	0.26	-0.16	16.89	7.39	864	6.98
2	Li-1NP	0.13	7.04	0.02	-0.11	-0.04	18.49	8.18	1082	7.67
3	Li-2NP	0.45	6.36	0.19	0.08	-0.01	15.89	6.84	1166	8.74
4	Li-2NP	0.24	6.57	0.02	-0.1	0.03	15.55	6.68	1159	8.78
5	Li-3NP	0.19	6.78	0.05	-0.07	0.08	17.69	7.77	1058	7.13
6	Li-3NP	-0.2	7.42	-0.26	-0.39	0.25	16.32	7.11	1094	7.40
7	Li-4NP	0.26	7.49	0.29	0.16	0.21	17.96	7.95	n/a	n/a

8. ESTIMATION OF THERMAL ENERGY FROM THE EXISTING GEOTHERMAL WELLS

The constructed production wells ensure 150 m³/h of geothermal fluids which produce thermal energy rate Et=3,841,300 kcal/h considering a reinjection (waste water) temperature (T_o) of 25°C. This thermal energy rate corresponds to thermal installed capacity of 4.47 MWt and is approximately equivalent to 3365 TOE/yr. In particular, the thermal energy rate (kcal/h), the installed thermal capacity (MWt) and the annual energy savings (TOE/yr) for each geothermal production well are as follows:

(i) Well Li-1P: thermal energy rate E_t=60,000 kcal/h, installed thermal capacity: 0.07 MWt and energy savings: 52.56 TOE/yr, assuming Q=4 m^3/h, T_w=40°C, T_o=25°C and $\Delta T=T_w-T_o$=15°C

(ii) Well Li-1NP: thermal energy rate E_t=412,500 kcal/h, installed thermal capacity: 0.48 MWt and energy savings: 361.35 TOE/yr, assuming Q=15 m^3/h, T_w=52.5°C, T_o=25°C and $\Delta T=T_w-T_o$=27.5°C

(iii) Well Li-2NP: thermal energy rate E_t=2,182,500 kcal/h, installed thermal capacity: 2.54 MWt and energy savings: 1911.87 TOE/yr, assuming Q=45 m^3/h, T_w=73.5°C, T_o=25°C and $\Delta T=T_w-T_o$=48.5°C

(iv) Well Li-3NP: thermal energy rate E_t=170,000 kcal/h, installed thermal capacity: 0.20 MWt and energy savings: 148.92 TOE/yr, assuming Q=5 m^3/h, T_w=59°C, T_o=25°C and $\Delta T=T_w-T_o$=34°C

(v) Well Li-4NP: thermal energy rate E_t=1,000,000 kcal/h, installed thermal capacity: 1.16 MWt and energy savings: 876 TOE/yr, assuming Q=80 m^3/h, T_w=37.5°C, T_o=25°C and $\Delta T=T_w-T_o$=12.5°C

9. CONCLUSIONS

The exploration campaign at the Lithotopos-Iraklia low enthalpy geothermal field contributed significantly to the understanding of the geothermal conditions of the area. Based on the results of the geophysical survey, a detailed imprint of the basement morphology was accomplished and principal tectonic structures were identified. The encountered temperatures reached 75°C, exceeding the highest temperature previously recorded by exploration boreholes in the field (62°C in borehole Li-4). A three

dimensional distribution of temperatures for the entire geothermal field was implemented and a probable upflow zone at the east bank of Lake Kerkini was identified. Additionally, the construction of four production wells contributed to the determination of the hydraulic characteristics of the geothermal resource, for which we had little information before. The chemical analysis of water and gas samples revealed geothermal fluids of good quality and low scaling and corrosion potential.

The geothermal waters produced from wells in the Lithotopos-Iraklia low enthalpy geothermal field can be used in various direct uses including small to medium sized greenhouse heating, pool heating, soil heating, balneology etc. Cumulatively, as mentioned above, the constructed production wells ensure 150 m^3/h of geothermal fluids which produce thermal energy rate Et=3,841,300 kcal/h corresponding to thermal installed capacity of 4.47 MWt. This thermal energy is approximately equivalent to 3365 TOE/yr.

The present study focuses on a small part of the Lithotopos-Iraklia geothermal field, corresponding to approximately the 30% of the total field extent. Further geothermal investigation is proposed to be done alongside the exploitation of the existing production wells, in order to expand the area and increase the geothermal potential of the field. The Municipality of Iraklia will soon submit the relative feasibility study with the proposed investments for the field development.

REFERENCES

Arnórsson, S., Gunnlaugsson, E., Svavarsson, H.,. The chemistry of geothermal waters in Iceland. III. Chemical geothermometry in geothermal investigations, *Geochimica et Cosmochimica Acta*, **47**, (1983), 567-577

Arvanitis, A.: Geothermal Study in the SW Part of the Strymon basin, *PhD Thesis*, Aristotle University of Thessaloniki, Thessaloniki (2003) (in Greek)

Arvanitis, A.: Preliminary Geothermal Investigation Northwest of Lake Kerkini, Strymon Basin, *Bulletin of Geological Society of Greece, Sp. Pub. 7.*, *Ext. Abs. GSG2019-191,* 15th International Congress of the Geological Society of Greece, Athens (2019).

Cooper, H.H. and Jacob, C.E.: A Generalized Graphical Method for Evaluating Formation Constants and Summarizing Well Field History, *Am. Geophys. Union Trans.*, **27**, (1946), 526-534.

D'Amore, F.: Applications of Geochemistry in Geothermal Reservoir Development, UNITAR/UNDP Centre on Small Energy Resources, United Nations Institute fur Training and Research, Rome; New York (1992).

Diersch, H.-J.: FEFLOW. Finite Element Modeling of Flow, Mass and Heat Transport in Porous and Fractured Media, Springer-Verlang Berlin Heidelberg (2014).

Eden, R.N. and Hazel, C.P.: Computer and Graphical Analysis of Variable Discharge Pumping Tests of Wells, The Institute of Engineers, Australia, Civil Engineering Transactions, (1973), 5-10.

Ellis, P.F.: A Geothermal Corrosivity Classification System, In: Geothermal Energy: The International Success Story, Transactions. Geothermal Resources Council. Geothermal Resources Council, Davis, California, (1981), 463-466

Etiope, G., Fridriksson, T., Italiano, F., Winiwarter, W., and Theloke, J.: Natural Emissions of Methane from Geothermal and Volcanic Sources in Europe, *Journal of Volcanology and Geothermal Research*, **165**, (2007), 76–86.

Fouillac, C., and Michard, G.: Sodium/Lithium Ratio in Water Applied to Geothermometry of Geothermal Reservoirs, *Geothermics*, **10**, (1981), 55-70

Giggenbach, W.F.: Geothermal solute equilibria. Derivation of Na-K-Mg-Ca geoindicators, *Geochimica et Cosmochimica Acta,* **52**, (1988), 2749-2765.

Karmis P.: Automatic interpretation of Transient EM surveys, *PhD Thesis*, Athens, Greece (2003)

Karydakis, G., and Kavouridis, T.: Geothermal Exploration in the Lithotopos-Iraklia Area During 1983, *Technical Report*, I.G.M.E., Athens (1984).

Karydakis, G., Kavouridis, T., and Vekios, P.: Additional Geothermal Exploration in the Areas of Iraklia, Sidirokastro and Ivira-Achinos in the Strymon Graben, *Technical Report,* I.G.M.E., Athens (2001).

Karydakis, G., Arvanitis, A., Andritsos, N., and Fytikas, M.: Low Enthalpy Geothermal Fields in the Strymon Basin (Northern Greece), *Proceedings*, World Geothermal Congress, Antalya, Turkey (2005).

Papic, P.: Scaling and Corrosion Potential of Selected Geothermal Waters in Serbia (No. 9), United Nations University - Geothermal Training Programme (1991).

Parkhurst, D.L. and Appelo, C.A.J.: Description of input and examples for PHREEQC Version 3-A computer program for speciation, batch-reaction, one-dimensional transport, and inverse geochemical calculations, (2013).

Piper, A.M.: A Graphic Procedure in the Geochemical Interpretation of Water-Analyses. *Transactions*, American Geophysical Union, **25**, 914-928, (1944).

Powell, T., 2000: A Review of Exploration Gas Geothermometry, *Proceedings*, Twenty-Fifth Workshop on Geothermal Reservoir Engineering, Stanford University, Stanford, California (2000)

Staikopoulos, G., Antoniades, P., and Matziaris, F.: Basic Geological Map of Greece: Kerkini map sheet, 1:50,000 scale, I.G.M.E., Athens (under publication).

Theis, C.V.: The Relation Between the Lowering of the Piezometric Surface and the Rate and Duration of Discharge of a Well Using Groundwater Storage, *Am. Geophys. Union Trans.*, **16**, (1935), 519-524.